EOL3 M0 X-Ray Tomography Test Results

R.Avramidou[2], Z.Banhidi[2], N.Bojko[1], A.Borisov[1], V.Goriatchev[1], S.Goriatchev[1],
V.Gushin[1], R.Fakhroutdinov[1], A.Kojine[1], A.Kononov[1], A.Larionov[1],
Yu.Salomatin[1], S.Schuh[2], Yu.Sedykh[2], A.Tchougouev,[1],
[1]Institute for High Energy Physics, 142280, Protvino, Moscow region, Russia
[2]CERN,CH-1211,Geneve 23,Switzerland

April 13, 2001

Abstract

Here we present results of X-ray tomography of the EOL3 M0 chamber. Peculiarities of the chamber X-ray tomography are discussed. Comparison of the tomography results with predictions of the production site measurements is made.

ATL-MUON-2002-009
20/06/2002

1 Introduction

EOL3 is one of the end cap chambers. It consists of 2 stair-case multi-layers (ML) (fig 1,2), each of 3 layers, 48 tubes/layer. Trapezoidal side has 14^o. Wire length (distance between the locators) varies from 3462 to 4062 mm with step 120 mm/stair. The chamber was assembled on beginning of November 2000 and shipped to CERN on November-December 2000. Installation for the tomography was done before Christmas of 2000, measurements were performed on 9-17 of January 2001.

Nominal parameters are given in table 1. These are average values. Together with averages, combined all production-site measurements (X-ray of wire in single tube, templates for combs, combs themselves, tube layers during the chamber assembling, sphere-blocks, stiff-back RASNIK monitors, distance between multi-layers) we created wire grid for both sides of the chamber similar to one which is result of the X-tomography (see [1]). EOL3 M0 was the first large end cap chamber at the X-tomography. The EC chambers are designed for using in vertical position and their spacer is not stiff. A priory it was waited for that the chamber placed at X-tomo horizontally will be bended and the bending will spoil the X-tomography results. Now it is really seen.

The X-ray tomography was developed for quality control of the barrel chambers. During several years of its operation some standard of data analysis was established. It based on using of grid-fit.

Here we show that the grid-fit can provide parameters of the large EC chamber if some corrections will be applied. Of course more carefull interpretation of the grid-fit results is needed as compare to barrel chambers.

2 Nominal parameters of the chamber

Table 1 presents the list of main nominal parameters provided before the tomography. The table contents average values. Variations of these parameters can be seen from the wire map, which was also provided.

3 RASNIK readings

Table 2 contents last in-plane RASNIK readings, taken on the granite table at finishing of the chamber assembling, and ones taken during X-tomography of the chamber at different flip orientations. As a reference

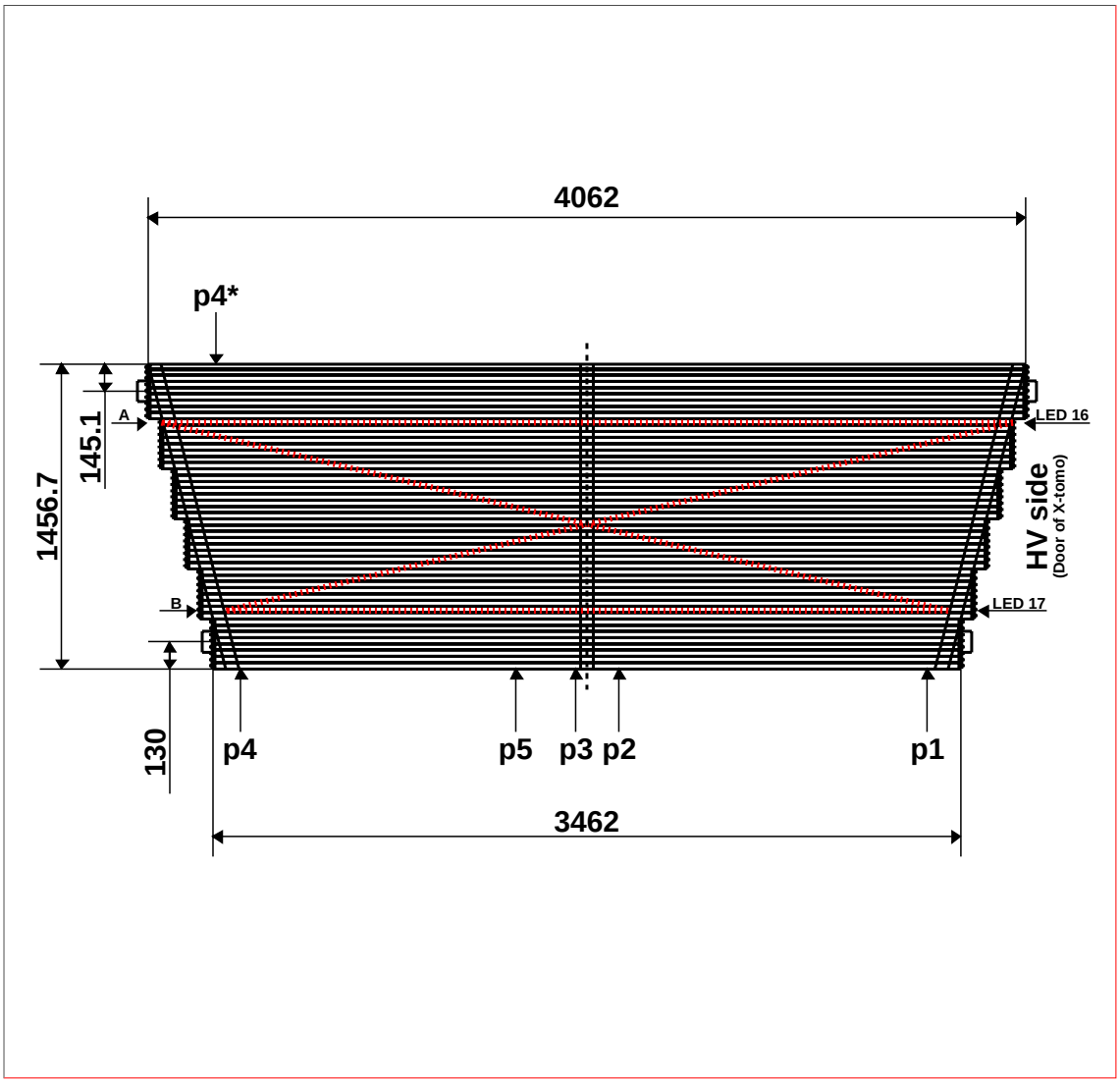

Figure 1: EOL3 top view as it was at r0 scan at X-tomo

Table 1: Average nominal parameters of EOL3 M0

Parameter name	Value	Tolerance
Z_{pitch},mm	30.035	0.0005
Distance between layers (Y_{pitch}),mm	26.011	0.005
Distance between multi-layers, mm	199.960	$^{+0.010}_{-0.020}$
Z-shift of middle layer,mm	-15.016	-
Relative Z-shift of multi-layers,mm	-0.010	-

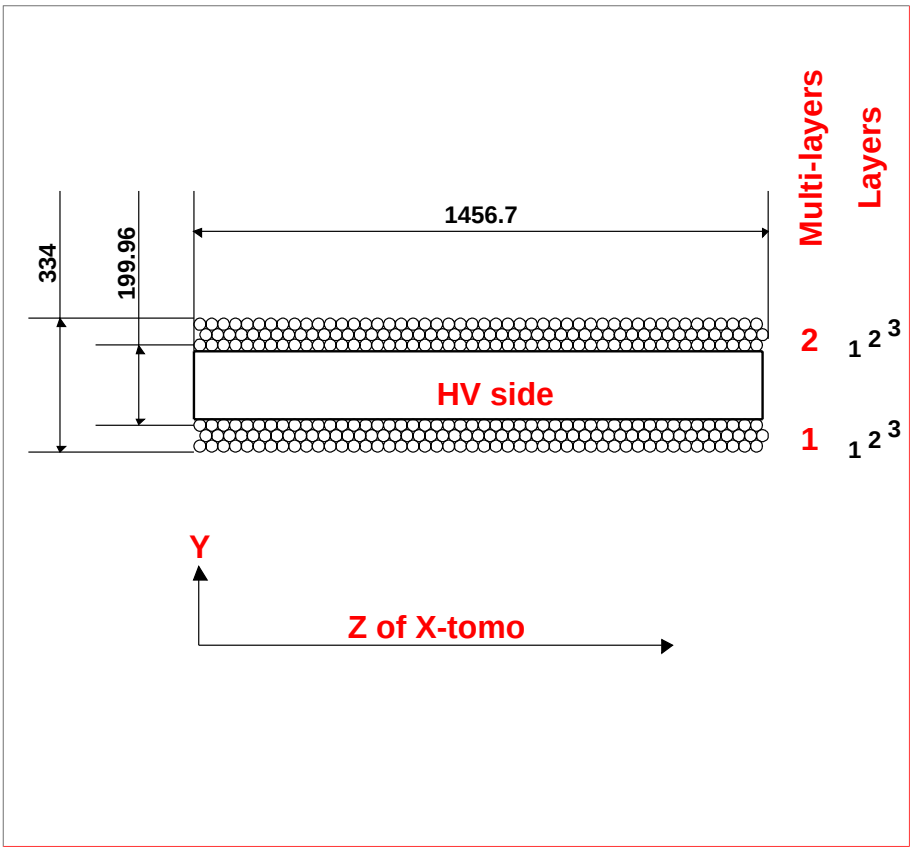

Figure 2: EOL3 cross-view as it was at r0 scan at X-tomo

Table 2: RASNIK readings data

CCD-LED	On table		Flip r0		Flip r1		Flip r2	
	Z,μm	Y,μm	Z,μm	Y,μm	Z,μm	Y,μm	Z,μm	Y,μm
A 16	53629	9588	53627	9940	53552	4195	53625	9898
A 17	70278	31417	70288	31783	70393	26321	70291	31693
B 16	51799	4318	51834	9576	51768	4057	51828	9594
B 17	65775	25561	65715	30598	65813	25411	65724	30576

Table 3: List of EOL3 M0 X-ray tomography scans

No	Scan number	St.d.[1] μm	St.d.[2] μm	St.d.[3] μm
1	**EOL_2001_01_p1_r0_106**	17.1	12.1	12.1
2	EOL_2001_01_p2_r0_107	16.2	12.6	13.1
3	EOL_2001_01_p3_r0_108	15.2	-	12.5
4	EOL_2001_01_p4*_r0_109	18.5	-	17.2
5	EOL_2001_01_p5_r0_110	17.1	14.4	15.1
6	**EOL_2001_01_p4_r1_111**	**27.3**	**21.6**	**20.2**
7	**EOL_2001_01_p1_r1_112**	19.3	15.8	12.9
8	**EOL_2001_01_p1_r1_113**	19.3	15.7	12.8
9	EOL_2001_01_p2_r1_114	19.8	14.4	12.1
10	**EOL_2001_01_p4_r1_116**	**26.1**	**20.3**	19.1
11	**EOL_2001_01_p4_r2_117**	**21.1**	**20.1**	19.8
12	EOL_2001_01_p4*_r2_118	**20.3**	-	19.4
[1] with nominal parameters without any corrections				
[2] with nominal parameters and taking into account wire sag and longitudinal bending (for Y_{wire})				
[3] calculation with all corrections				

to naming convention of CCD-LED see fig.1, where positions of CCDs and LEDs on the cross-plates are shown. Point-dashed lines are light rays.

From the RASNIK data we concluded that average longitudinal sag of the chamber at X-tomo was about 1.25 mm. This value was used for all corrections and estimations which will be presented below.

4 List of X-tomography scans

12 scans of the chamber were performed. List of the scans is presented in table 3, which gives scan numbers and standard deviations of the grid fit with nominal parameters: without any corrections; with taking into account wire sag and influence of longitudinal bending on Y-coordinate of wires and with all known at this moment corrections (wire sag with nominal tension, chamber longitudinal bending with sag 1.25 mm, transverse sag of the chamber 23 μm and coherent shift of layers due to longitudinal bending and trapezoidal side).

Scan naming conventions: **p1-p5** are positions of the X-tomography scan along the chamber (shown by arrows in fig.1); **r0** means original orientation of the chamber, as it was in the box; **r1** is flipped orientation and **r2** is the same as **r0** but after two rotations.

Due to misunderstandings 3 scans were done at wrong positions: at **p3** a lot of wires were lost due to the lenses holder; at position **p4*** the shortest tube stair was lost. Scans closed to ends of tube are more interesting: **106, 111, 112, 113, 116, 117** (for simplicity we shall use in future only last 3 digits from scan name).

5 Peculiarities of end cap chambers at X-ray tomography

Due to change of stairs length wire sag in each stair is different. It can be easy calculated from known wire tension and length.[1] Before the chamber assembling the tension all tubes was measured [4], but in this work we always used the nominal tension 350 g.

[1]Due to lack of good wire we were forced to introduce into the chamber the tubes with tension outside of specified limits. Real tension can be taken from DB, we used it for production of our wire map [1,4].

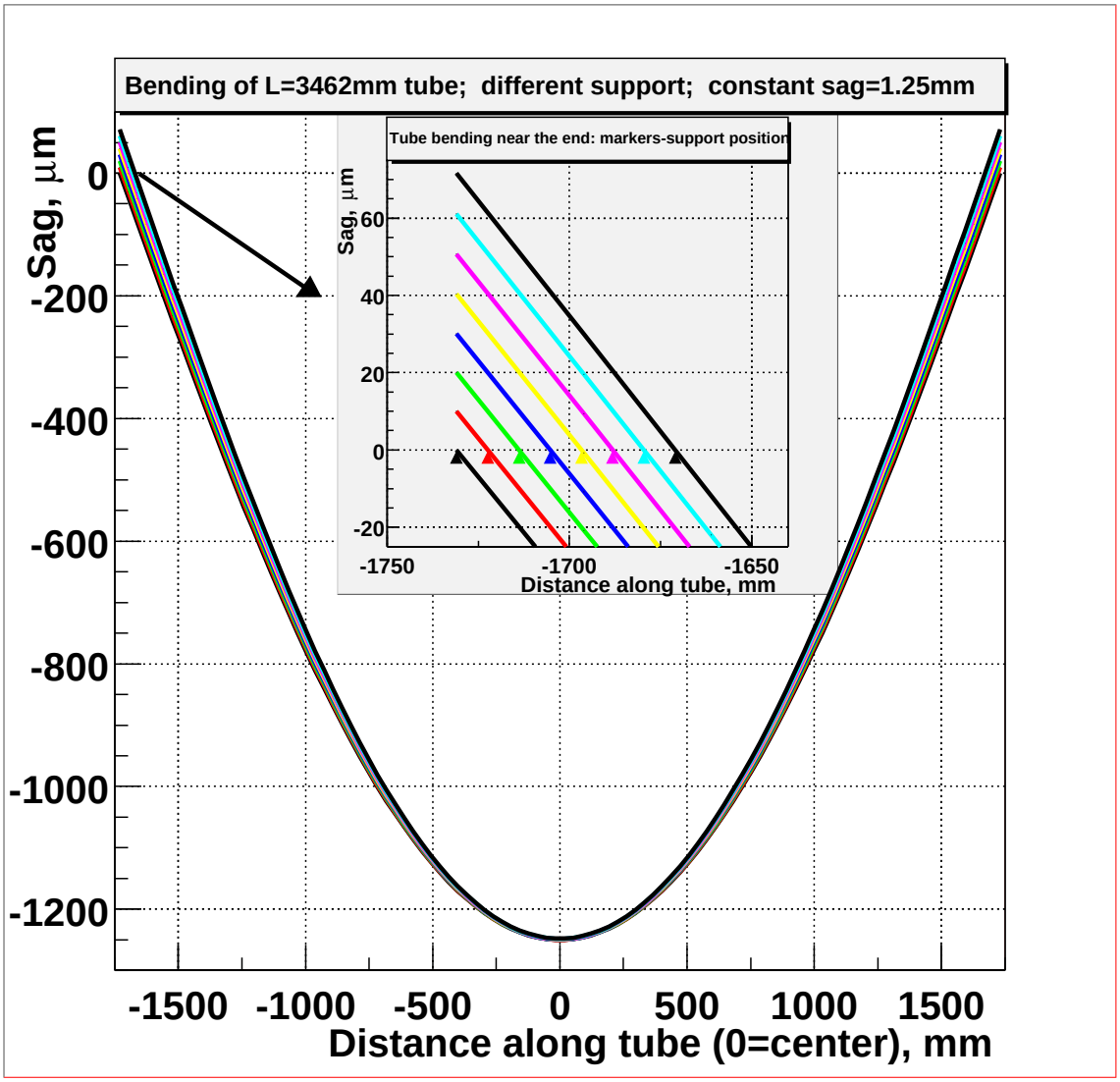

Figure 3: Tube curvature at constant sag=1.25mm and displacement of supports. In insertion the supports are shown by marker.

Due to poor stiffness of the spacer frame the chamber installed at the X-ray tomograph horizontally is bended both in transverse (YZ-plane) and longitudinal (YX-plane) directions.

Influence of the transverse bending on wire position is evident but unfortunately we have not inputs(at least now) for estimation of it except of results of X-ray tomography itself.

Contribution of longitudinal chamber bending into wire location is not so evident and we give here more wide explanation. Let us consider a tube which is supported at the ends. If the supports will displaced towards middle of the tube the ends of tubes will become higher. As an example in fig 3 calculated tube (L=3462) curvature is shown for the cases when displacement of the supports towards the middle of the tube is 0-60mm (length of our chamber stair) and sag is kept constant 1.25 mm. Zooming of the tube end is presented in inserted picture. Displacements of the supports shown in fig.3 correspond to length of tubes in stair outside of cross-plate (see fig.1). Thus within of each stair we are waiting for variation of vertical position of wire like one shown in zoom of fig.3.

At analysis of X-tomo data we must take into account wire sag, longitudinal and transverse bending. Calculated for scan position **p1** relative wires Y-coordinate within a layer are shown in fig.4. Calculation was done with 350 g tension and longitudinal chamber sag 1.25 mm; transverse bending band was extracted from X-tomo data.

Non-coherent behaviour of Y-coordinates of wires within of a cross-section is main difference of end cap chambers from barrel one. If for barrel chambers wire mesh in cross-section is rectangular, for end cap chamber it looks like parallelogram, long side of which has "saw"-shape with superimposed parabola due to transverse chamber sag. Summary of the differences:

- Wire grid in plane YZ looks like parallelogram due to wire sag difference;
- Y-coordinates follow "saw"-like shape due to the chamber longitudinal bending;
- Y-coordinate of wires follow to transverse bending;
- Due to the transverse sag Z-pitch at top will be shorter, as compare to one at the bottom of the chamber;
- Longitudinal bending through trapezoidal angle will induce Z-shift of layers, coherent for all wires within a layer.

6 X-tomo results for EOL3 in "barrel" mode

.

The first results of X-tomo for EOL3 M0 were presented in "barrel standard", when the peculiarities of the end cap chamber were not taken into account at all. We show in fig.5,6 residuals versus position of tube within a layer for grid-fit with nominal parameters for two scans: 106(the best) and 111(the worst), where different markers and colours correspond to 6 different layers of the chamber:

- (black(full cycle)-ML1/L1;
- red(full squares)-ML1/L2;
- green(full triangle up)-ML1/L3;
- blue(full triangle down)-ML2/L1;
- yellow(open cycle)-ML2/L2;
- rose(open squares)-ML2/L3).

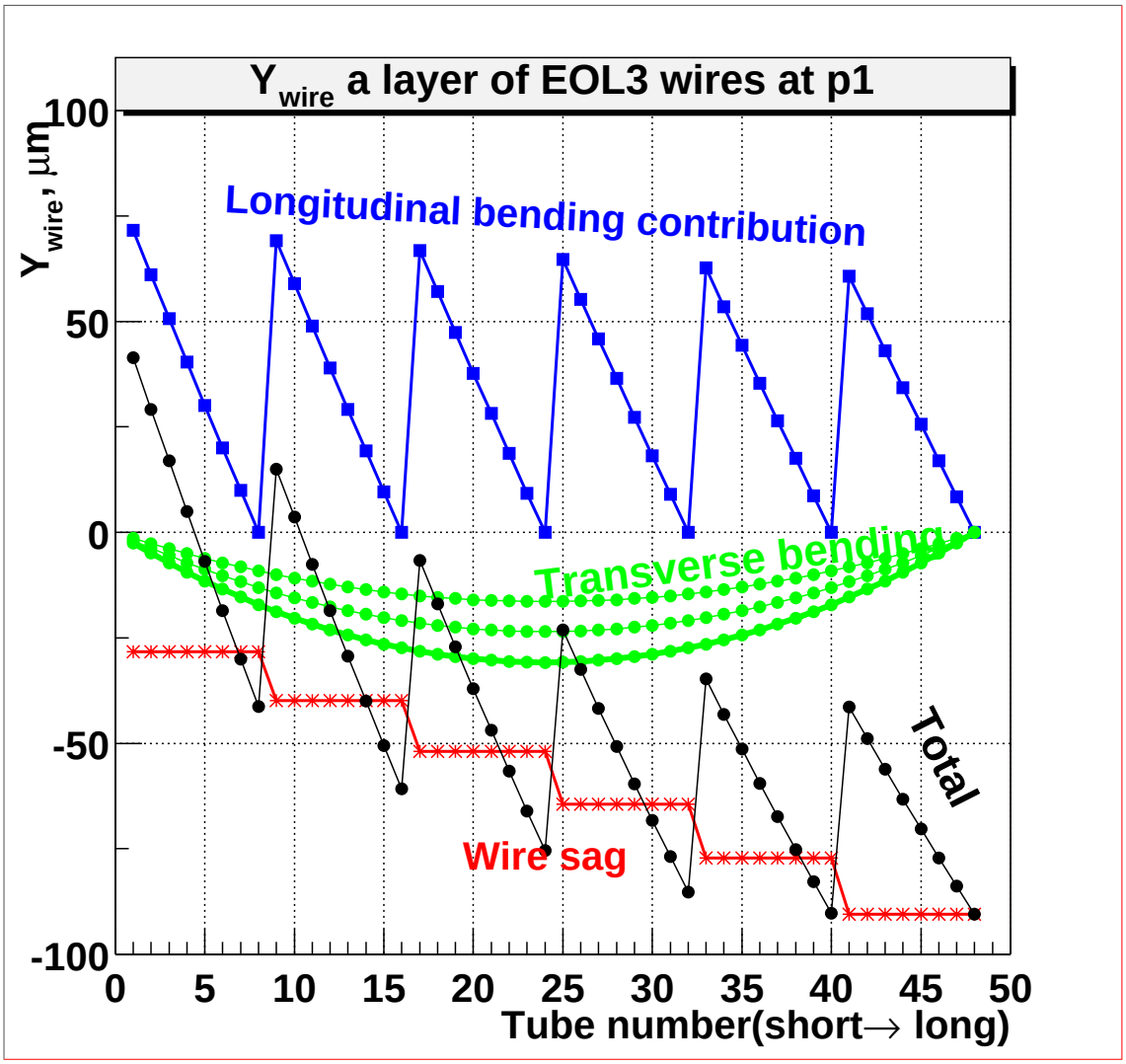

Figure 4: EOL3 Y-coordinate of wires at p1

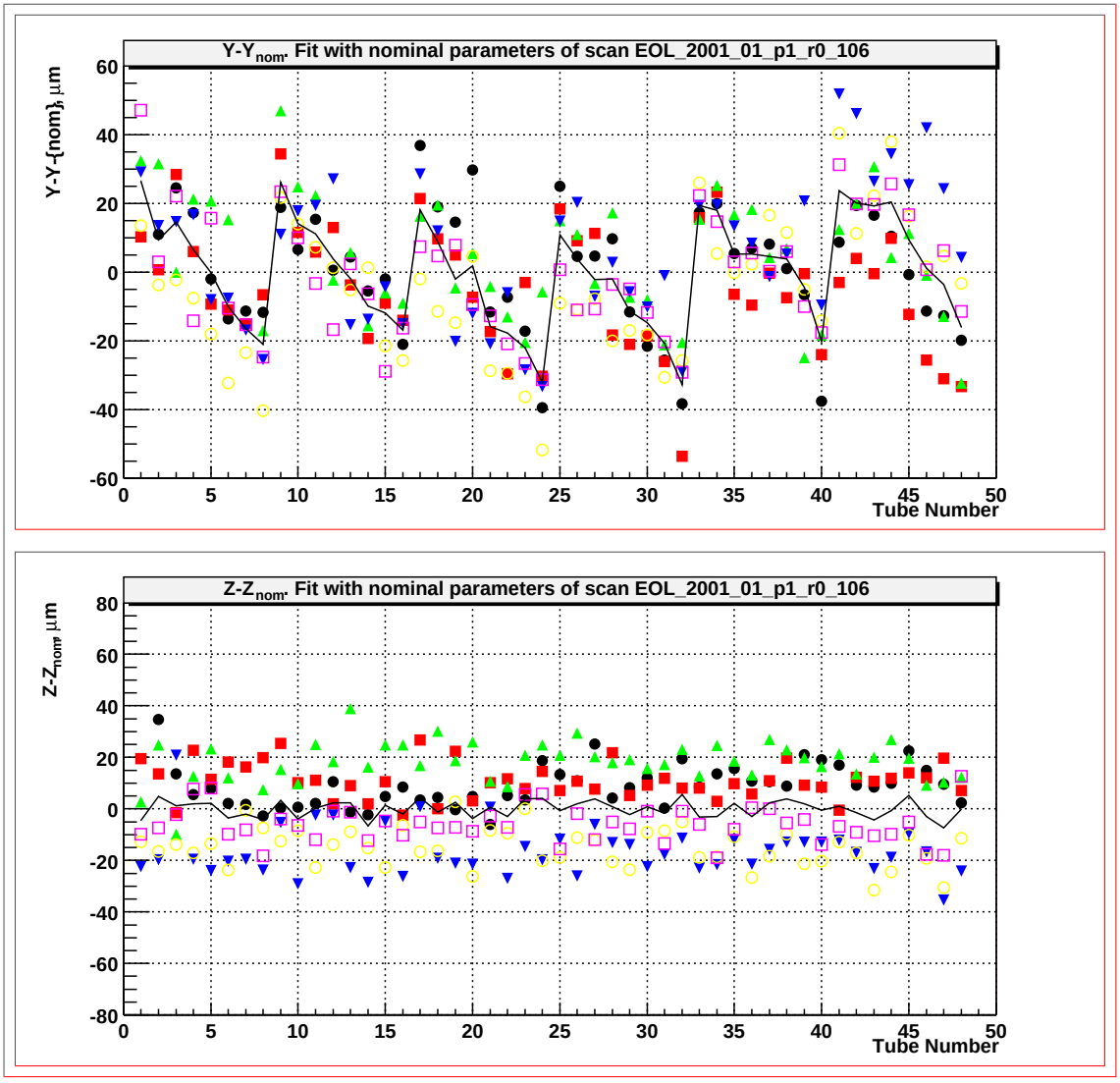

Figure 5: Scan 106. Residuals Y-, Z-coordinate for grid-fit with nominal parameters(barrel-manner)

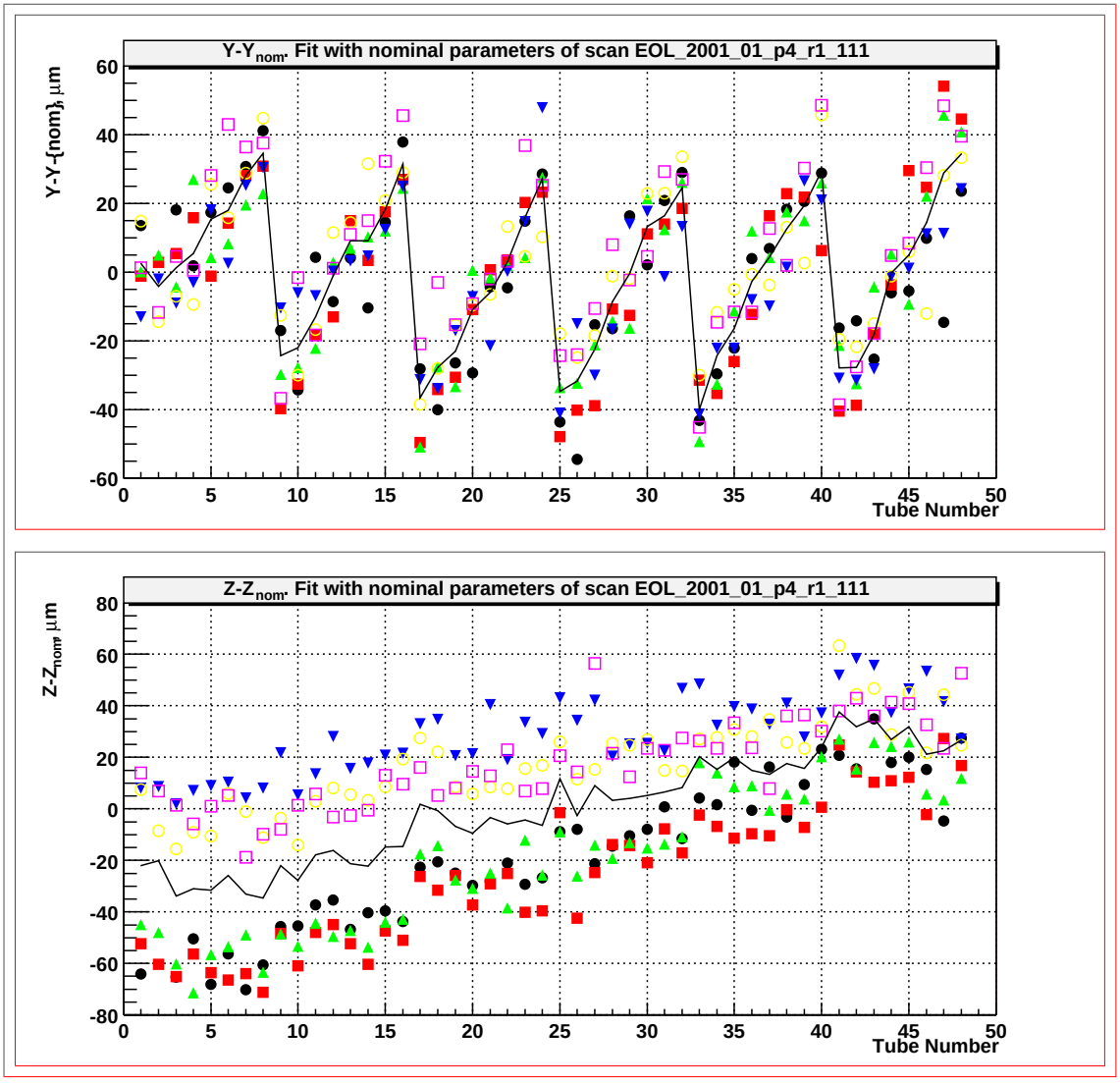

Figure 6: Scan 111. Residuals Y-, Z-coordinate for grid-fit with nominal parameters(barrel-manner)

Table 4: Transverse sag of the chamber

Scan	106	112	113	111	116	117	Average
Sag, μm	16.4	30.8	30.3	18.6	17.6	26.8	23.4
Position and flip	p1 r0	p1 r1	p1 r1	p4 r1	p4 r1	p4 r2	

Black line in fig.5-6 presents simple average over 6 layers.

From fig.4-6 it is clearly seen that using of "barrel chambers standard" of presentation X-tomo data is not acceptable, at least in case of long end cap chambers. "Saw"-shape is well distinguished.

Seen these results X-tomo group was forced to correct Y-coordinate of wires taking into account the wire sag and longitudinal chamber bending. As inputs the nominal tension and average chamber longitudinal sag 1.25 mm were used. Results of grid-fits with such correction are also given in [2] and in Appendix.

Standard deviation for the grid fit with nominal parameters was improved. For the best scan it became 12.1 μm, but 3 scans at RO side are still out of specification.

7 Transverse sag of the chamber

To show more clear the transverse sag of the chamber we eliminated "saw"-shape and wire sag from Y-residuals and as result we have got curves shown in fig.7,8.

In fig.7-8 **AMPL** means the sag extracted from the 2nd power polynomial fit(full line) of average over 6 layers residuals. Summary for transverse sag is given in table 4. Average for scans near ends of the chamber is 23 μm. Difference the sag at the chamber flipping is explained by the sag "frozen" into the chamber. For RO side the sag about 10μm was already seen at the chamber assembling (fig.28-33 in ref.[1]).

8 Reproducibility of X-tomo results

There were several scans taken at the same cross-section of the chamber (or very close, like scans at positions p2 and p3) and at the same flip-orientation. These scans provide us nice opportunity to check X-tomo reproducibility and wire resolution by means of simple comparison of the same wire coordinates measured at different scans.

Table 5 presents results of such comparison. It contents average and RMS of difference for wires coordinates measured in two scans. Upper layer of top multi-layer was used as a reference to connect two scans grids.

Two pairs of scans 112-113 and 111-116 were done almost at the same place along the chamber. From their comparison we have:

- top multi-layer (Y,Z) σ_{wire}=2.2 μm, systematic$<$ 1.0μm
- bottom multi-layer (Y) σ_{wire}=4.2 μm, systematic $<$ 1.0μm
- bottom multi-layer (Z) σ_{wire}=2.8 μm, systematic is $\pm$2.5μm

It is close to X-ray tomography calibration results/3/, where 2 μm errors were reported both systematic and statistical. Due to presence of material we see worse results for bottom multi-layer. 2.5μm systematic for Z-direction can be explained by temperature effect.

For pair of scans 117-118 average difference about 8 μm is for Z of bottom ML. Scan 118 is specific scan with 15% fraction (1 stair) of lost wires. Probably such difference is caused by grid-fit for chamber with transverse curvature.

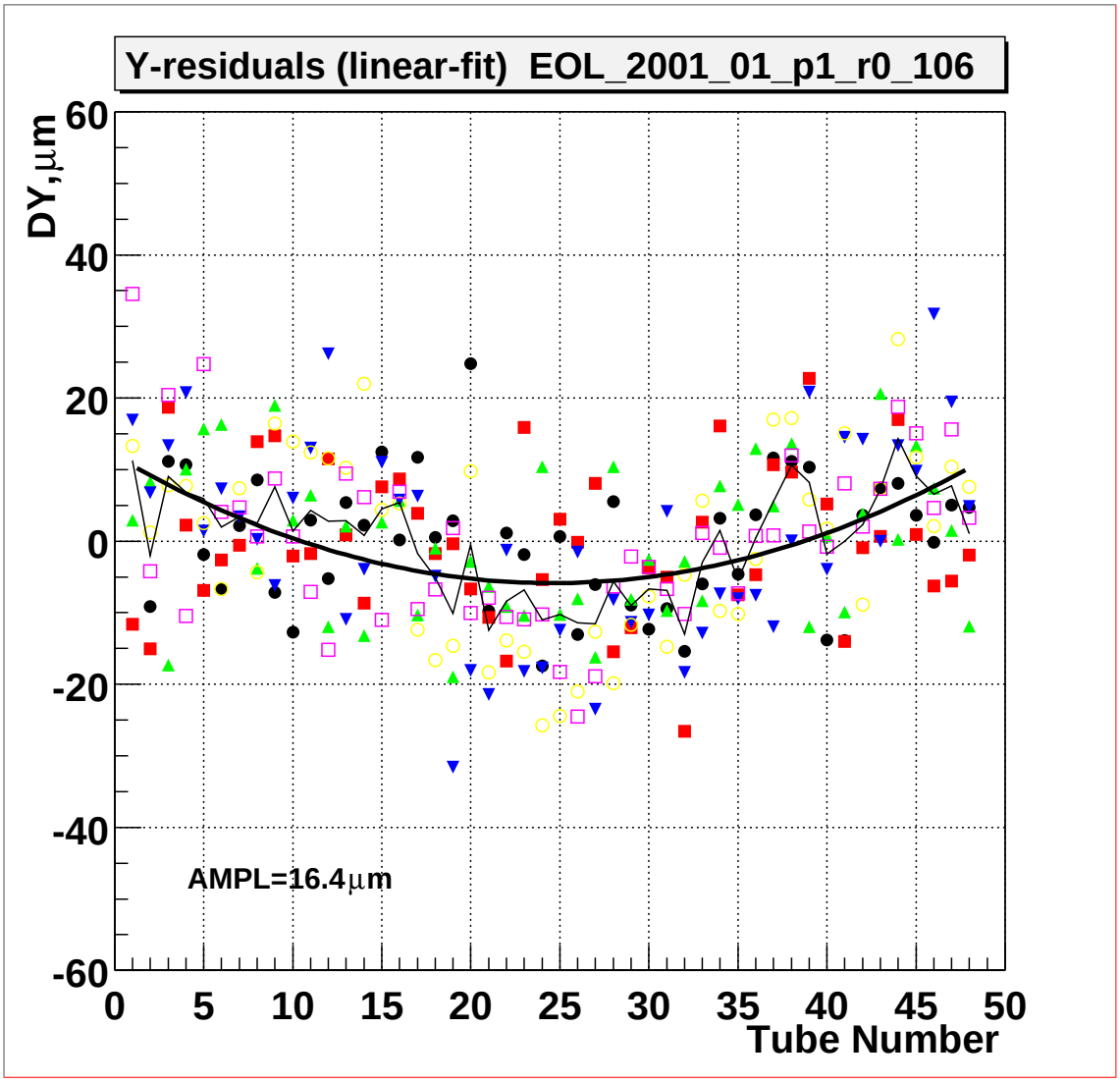

Figure 7: Scan 106. Y-residuals for grid-fit with nominal parameters; wire sag and tube bending are corrected.

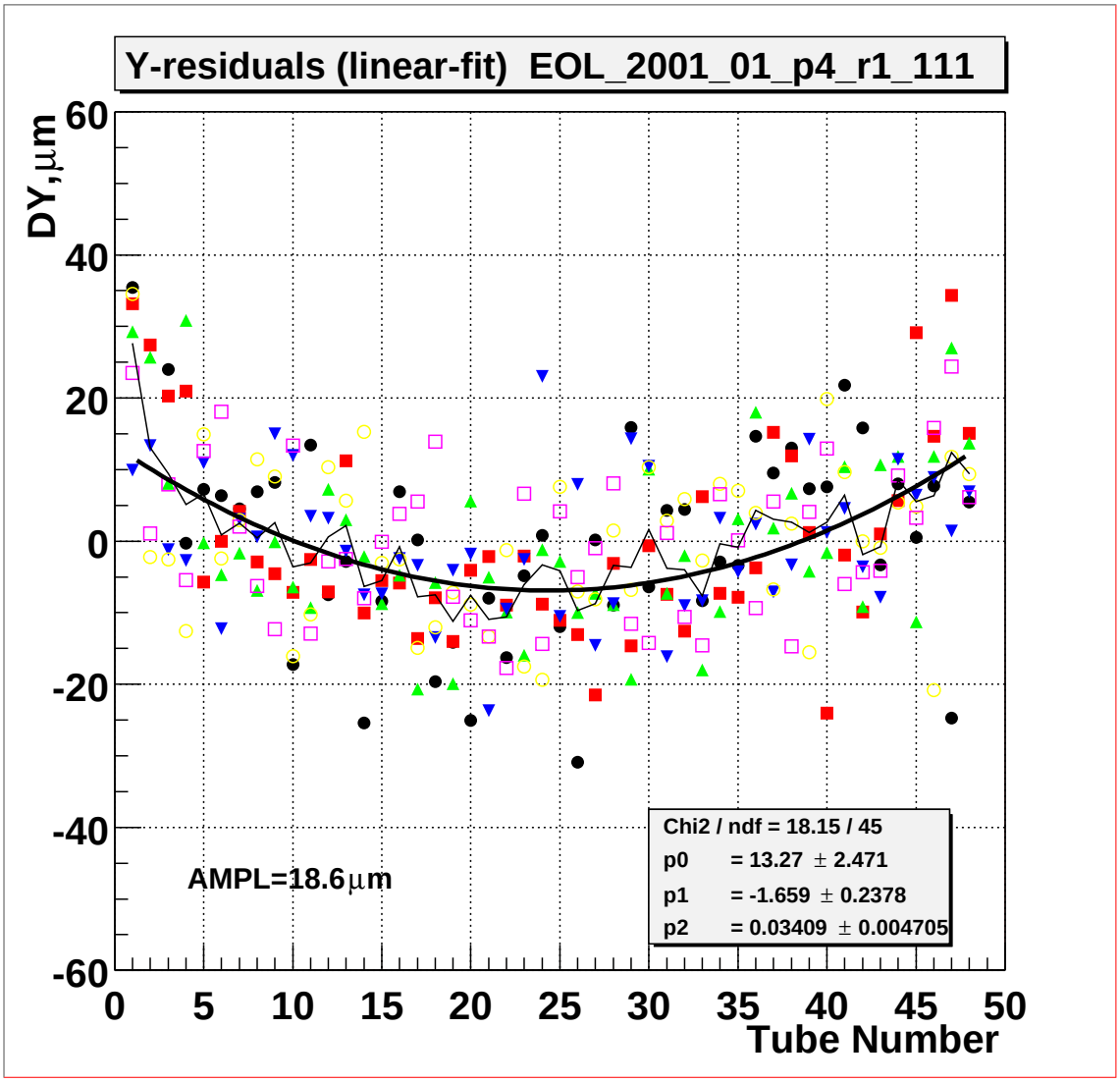

Figure 8: Scan 111. Y-residuals for grid-fit with nominal parameters; wire sag and tube bending are corrected.

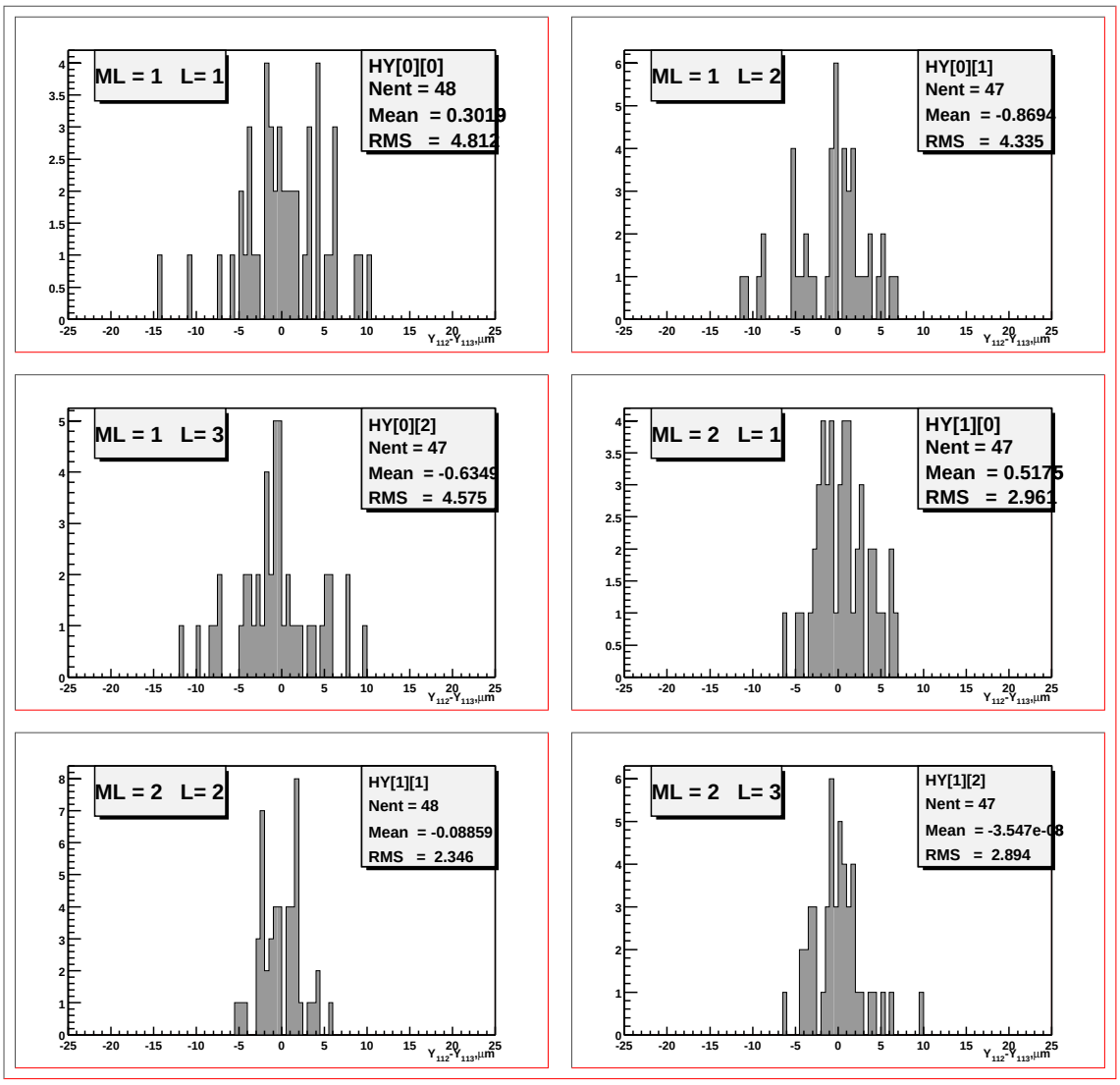

Figure 9: Difference of Y-coordinate of wires measured at the same position of the chamber (scans 112-113)

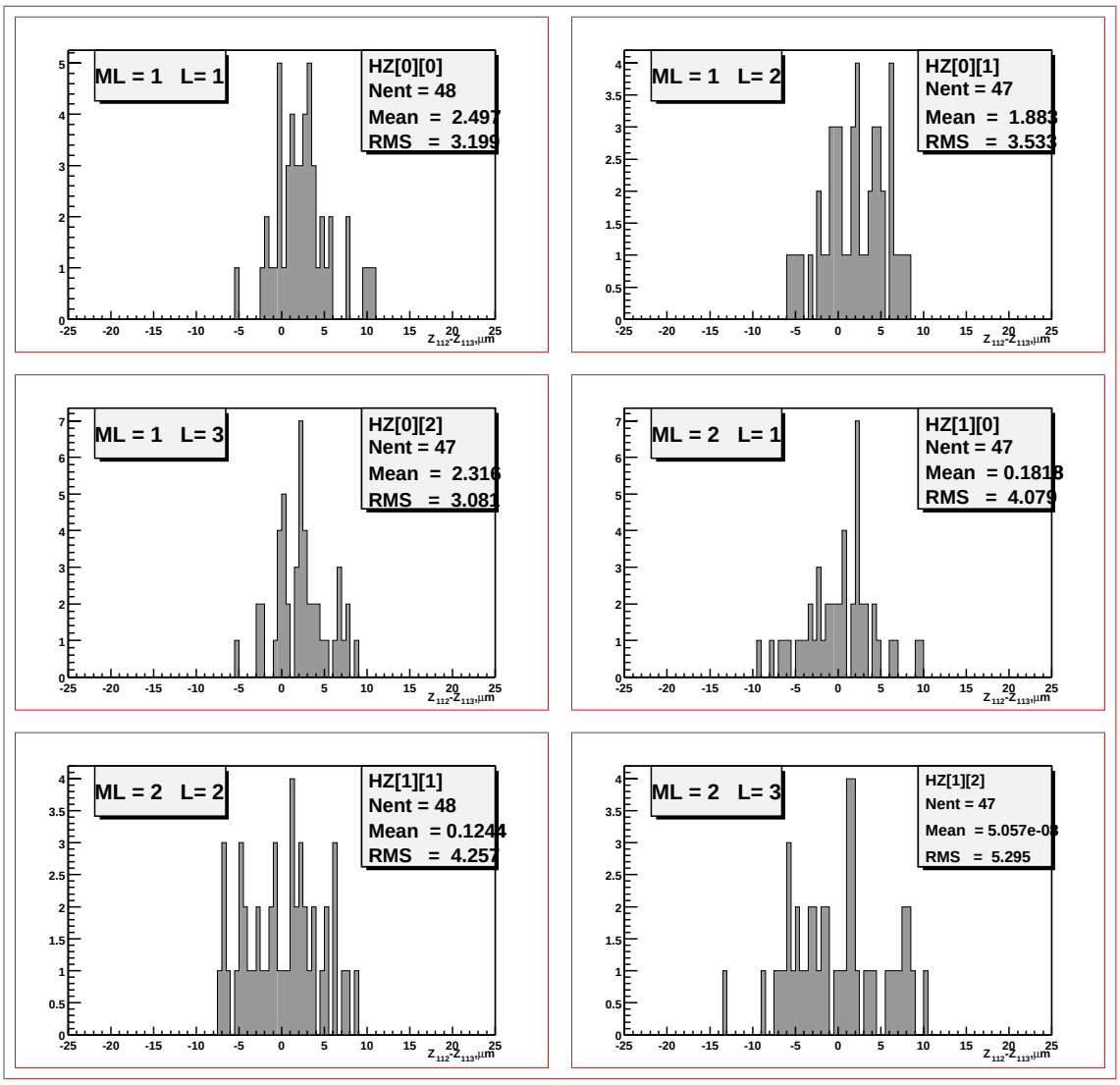

Figure 10: Difference of Z-coordinate of wires measured at the same position of the chamber (scans 112-113)

Table 5: Reproducibility of X-tomo (all values in μm)

	ML	L	**112-113**		**111-116**		107-108		107-110		117-118	
			Mean	RMS	Mean	RMS	Mean	RMS	Mean	RMS	Mean	RMS
Z	1	1	2.5	3.1	-2.4	2.9	4.1	3.5	3.7	5.1	9.2	4.1
		2	1.9	3.5	-2.1	2.8	2.4	4.4	2.3	5.6	8.5	5.6
		3	2.3	3.1	-2.4	3.0	4.0	3.7	3.6	5.6	7.3	5.8
	2	1	0.2	4.1	-0.9	2.8	1.4	3.6	1.5	5.6	2.2	6.3
		2	0.1	4.3	-0.6	3.4	-0.8	4.1	-1.5	6.7	0.8	6.8
		3	0.0	5.2	0.0	3.8	0.0	4.9	0.0	7.6	0.0	7.3
Y	1	1	0.3	4.8	0.4	4.7	2.4	4.6	1.8	4.8	1.3	6.3
		2	-0.9	4.3	0.4	4.9	3.2	4.8	2.3	5.2	2.1	7.1
		3	-0.6	4.6	1.7	4.6	0.8	4.5	-0.4	4.7	2.3	6.9
	2	1	0.5	3.0	0.5	4.0	-0.6	3.1	-0.4	4.5	0.0	8.2
		2	-0.1	2.3	0.6	2.6	-0.1	2.7	-0.5	3.7	0.2	8.7
		3	0.0	2.9	0.0	2.5	0.0	3.9	0.0	3.8	0.0	7.4

Table 6: Correlation X-tomo and designer results

Scan number	cor_Y	cor_Z
EOL_2001_01_p1_r0_106	0.25	0.76
EOL_2001_01_p2_r0_117	0.41	0.66

9 Comparison wire maps of chamber builders and X-tomo

9.1 Wire coordinate correlation

Comparison was done on 'wire-by-wire' basis because of almost all wires were measured by X-tomo. It allows us to attribute X-tomo wire grid to "physical" wires in the chamber.[2] In fig.11,12 Z-residuals are shown for scan 106 and 206(prediction of builders wire map for position corresponding to X-tomo scan 106).

Large residuals in fig.11-12 are inclosed in cycles. These are "key"-wires to validation of coincidence of the wires maps. It is not trivial task due different naming conventions[3]. For comparison of two maps we calculated correlation coefficient (cor): cor= $\sum_{k=1}^{n} \frac{\delta_{ik} \cdot \delta_{jk}}{n \sigma_i \sigma_j}$, where δ_{jk}, δ_{ik} are residuals and σ_j, σ_i are standard deviations for two sets of measurements (i,j) which are compared. Table 6 presents the correlation coefficients for two scans, average for 6 layers. For calculation of residuals of X-tomo data was done linear fit with correction of wire sag and the longitudinal bending. Transverse bending corrections were not applied therefore Y-correlation is less.

9.2 Multi-layer separation

Value of multi-layers separation given in X-tomo grid-fit tables is average one. Difference of Y-coordinate of wires with the same numbers in ML=1 L=3 and ML=2 L=2 can show behaviour of the multi-layers distance across the chamber and provides also additional possibility to compare design parameters with measured one (see fig.13,14).

[2]Let us remind, that wire map which is result of the X-ray tomography contents wires numbers which do not correspond to position of wires within a layer. In case of lost wires from both sides of the chamber it is impossible to attribute X-tomo wire map to real wires!

[3]At flipping of the chamber its " physical" layers change place and numbers of wires are swapped.

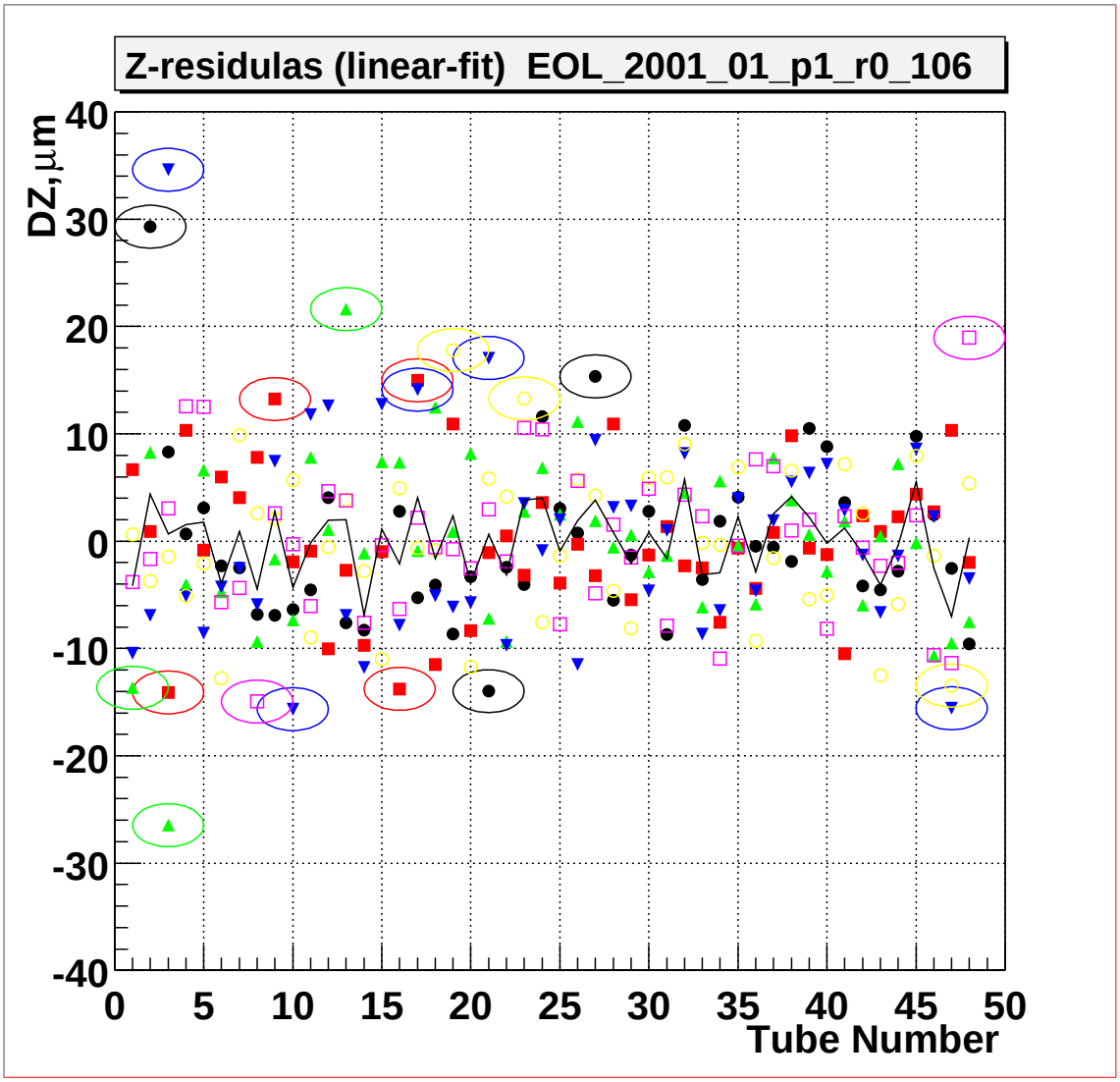

Figure 11: Residuals of Z-coordinate of wires measured at scan 106

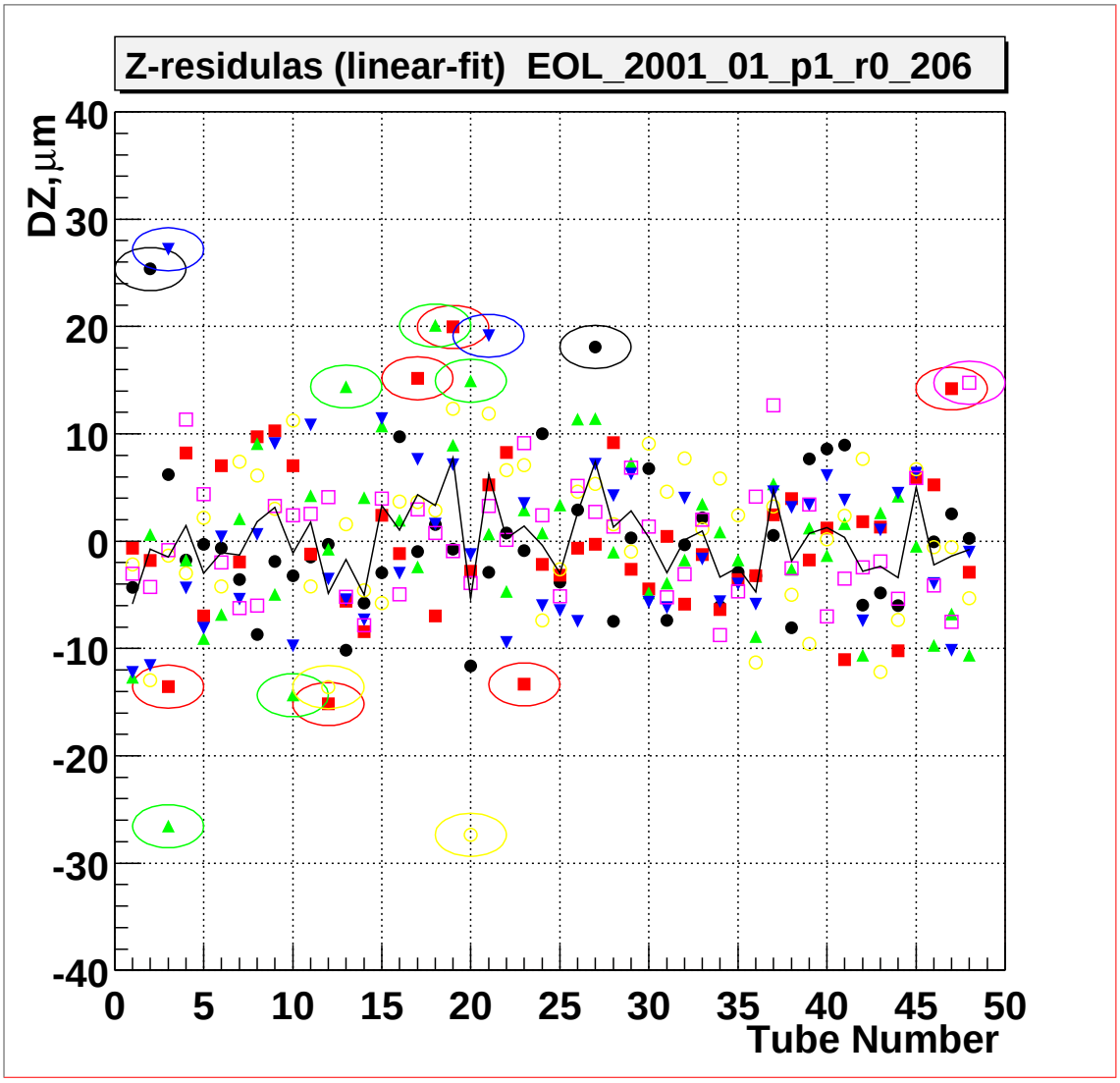

Figure 12: Residuals of Z-coordinate of wires predicted from design values for scan 106

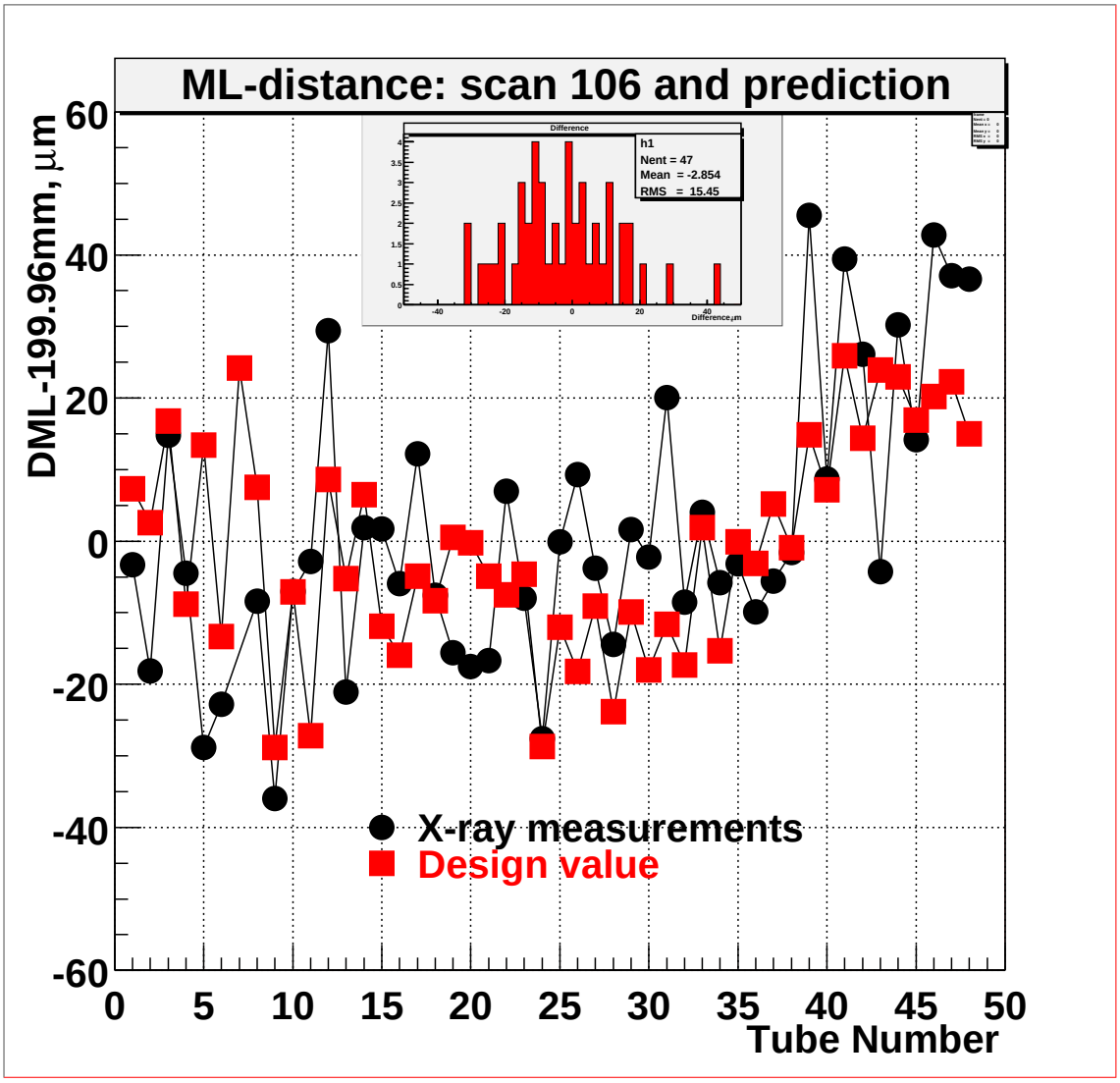

Figure 13: Distance between multi-layers across the chamber: X-ray results and our data near HV side

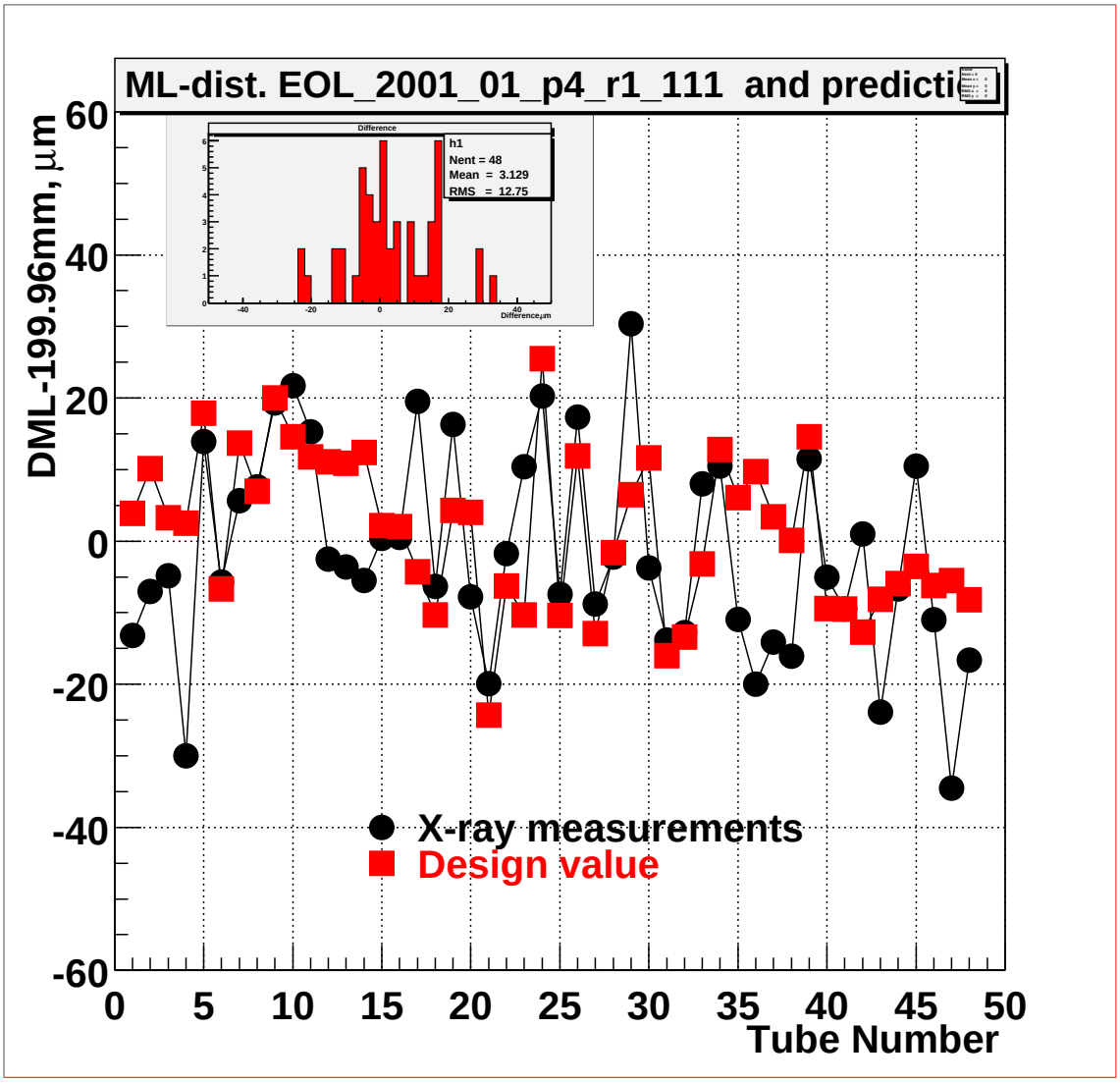

Figure 14: Distance between multi-layers across the chamber: X-ray results and our data near RO side

Table 7: Y-shifts of neighbour layers

	ML 1		ML 2	
	L3-L1 -52.022mm			
Scan	Mean	RMS	Mean	RMS
106 r0 HV	3.3	13.6	-6.9	15.4
112 r1 HV	-7.9	13.3	-2.6	15.1
113 r1 HV	-7.2	16.3	-1.8	15.8
111 r1 RO	-0.8	14.0	8.4	14.4
116 r1 RO	-1.1	15.0	9.0	13.8
117 r2 RO	13.2	14.0	0.6	15.8
	L2-L1 -26.012mm			
Scan	Mean	RMS	Mean	RMS
106 r0 HV	-6.7	11.1	-12.1	14.8
112 r1 HV	-5.0	12.6	-0.6	15.3
113 r1 HV	-4.5	12.0	0.1	16.3
111 r1 RO	-3.4	14.3	3.9	14.1
116 r1 RO	-2.6	14.2	3.9	13.9
117 r2 RO	-2.7	15.2	-5.7	12.9
	L3-L2 -26.012mm			
Scan	Mean	RMS	Mean	RMS
106 r0 HV	8.3	15.2	3.2	12.1
112 r1 HV	-4.6	12.4	-4.8	12.2
113 r1 HV	-4.3	12.2	-3.9	12.4
111 r1 RO	0.4	11.3	2.4	14.5
116 r1 RO	-0.7	12.9	3.0	14.7
117 r2 RO	13.9	13.4	3.1	14.4

Difference between X-tomo and builders data (inserted histograms in fig.13,14) is -2.9±15.5(RMS) μm for HV side and 3.1±12.8(RMS) μm for RO side. Our fall during the chamber lifting accident[1] is clearly seen in fig.13 at HV side as a 20 μm kink at the last stair. Below the last stair the distance is: -4.2±15.4(RMS) μm from X-tomo and -6.1±11.6(RMS) μm; for last stair it is 27.8±14.5(RMS) μm and 20.2±4(RMS) μm, X-tomo and producer data respectively.

Similar comparison of flipped scans at the same chamber section gives, for instance, follow multi-layer distance difference: -3.3±7.0(RMS) μm(117 and 111 scans) and -7.8±8.6(RMS) μm(106 and 112 scans), which are close to results of grid-fits(see [2]).

10 Separation(Y-distance) of layers

Table 7 contents vertical separation of layers made on "tube-by-tube" basis. From data given in the table 8 we produced average for each side (results see in table 11).

11 Z-shifts of internal layers

Nominal value of Z-shift of internal layer is equal to half of Z-pitch. Measured by producers Z-shift of middle layers is 15.016mm and 15.022mm for HV and RO sides, respectively. From X-tomo wire map we calculated this shift as z-distance of the i-th wire of middle layer from line connecting wires with the same number in extreme layers. An example of such difference distribution is shown fig.15: for ML1(upper histogram), ML2(middle)

and total(bottom) for scan 106. In table 8 parameters of middle layer Z-shift distributions are summarised for

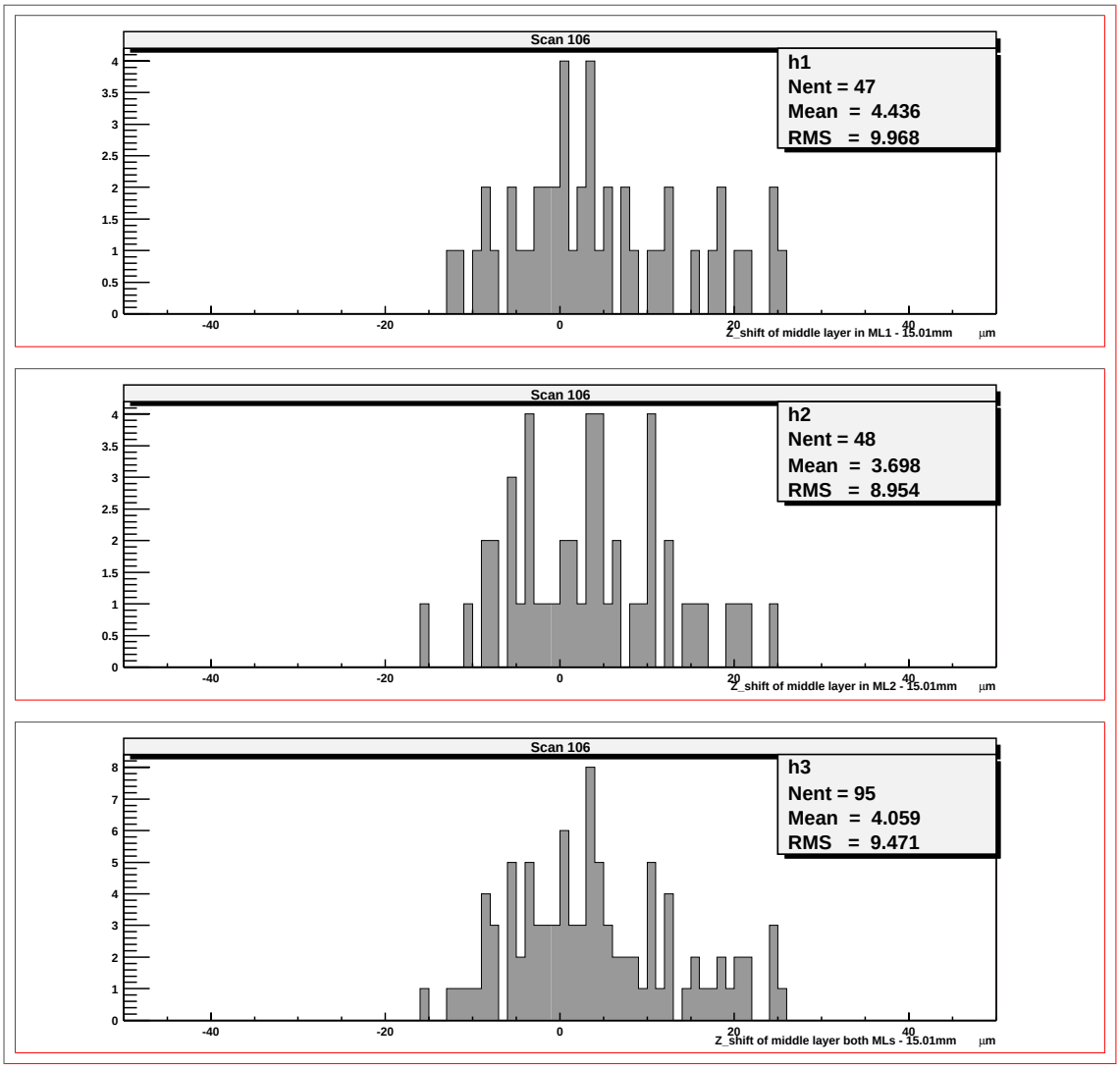

Figure 15: Scan 106. Distributions of z-shift of middle layer.

several scans. The 1st column shows scan number, flip orientation and side of the chamber. Numbers 206,217 are producer grid data. Taking averages we have got from X-tomo results Z-shift of middle layer:
HV side 15.014±0.001mm (design value 15.016mm);
RO side 15.024±0.001mm (design value 15.022mm). These estimations are slightly dependent on the chamber bendings, but we ignored them here.

Table 8: Z-shift of middle layer

	ML 1		ML 2		Total	
Scan	Mean	RMS	Mean	RMS	Mean	RMS
106 r0 HV	4.4	10.0	3.7	9.0	4.1	9.5
117 r2 RO	12.7	10.5	14.9	9.7	13.8	10.2
112 r1 HV	3.9	9.0	4.9	9.9	4.2	9.5
113 r1 HV	3.1	8.7	6.3	11.2	4.7	10.2
111 r1 RO	14.4	9.2	13.5	9.7	14.0	9.5
116 r1 RO	14.6	9.6	13.3	9.6	14.0	9.6
206	6.9	9.2	4.4	8.9	5.6	9.1
217	11.0	9.9	11.6	8.1	11.3	9.0

Table 9: Relative Z-shift of ML

Scan	106	112	113	111	116	117
dZ μm	-13.2	-10.9	-8.8	28.3	26.0	15.4
Position and flip	p1 r0	p1 r1	p1 r1	p4 r1	p4 r1	p4 r2

12 Z-shift of layers and multi-layers from nominal position

In Table 9 relative Z-shift of ML extracted from grid-fit is given. For HV side we see dZ near -10 μm independently on flip.

For estimation of Z-positions of layers we have to take into consideration influence of the chamber bending on Z-shift of layers

12.1 Influence of longitudinal bending on relative Z-shift of layers

Longitudinal bending will lead to change of wire locator position along X-direction (dX). For two layers we have got difference of X-coordinates of the locators: dX=$Y_{ij}\cdot\alpha$, where α is longitudinal bending angle near end of layer, Y_{ij}-separation of layers. Due to trapezoidal angle this shift will give contribution into coherent Z-displacement of whole layer. For instance, the second layer wrt. the 1st one will be shifted by $dZ_{12}=\pm tan(14^o)\cdot dY_{12}\cdot\alpha$, where sign depends on the flip orientation, Y_{12}-layers separation (26.012mm) and α is about 1.5mrad. Thus $Y_{12}=\pm 9.7$ μm and $Y_{13}=\pm 19.4$ μm. To check these estimation we calculated distribution of z-distance of wires in tube wrt. line connecting wires with same numbers in layer 2 of ML1 and ML2. For this calculation internal layers were shifted by 15.014(0.24)mm. Results are shown in fig.16,17. Statistical error of each point in fig.16,17 is about 1-1.5 μm.

For HV side within of 1-2μm uncertainty we can conclude that relative z-shift of layers (fig.16) is caused only by the longitudinal bending contribution. relative shift of multi-layers is equal to 0.

For RO side interpretation is not so clear. We can not exclude relative shift of ML at about 10 μm. Interpretation is difficult.[4]

Measured Z-shifts (fig.16,17) is 10% below of our estimation from the longitudinal bending.

[4]The same can be told about dZ given in grid fit, it can be due to shift of origin(beginning) of the multi-layer or due to Z-pitch variation. In case of EOL additionally there is longitudinal bending contribution.

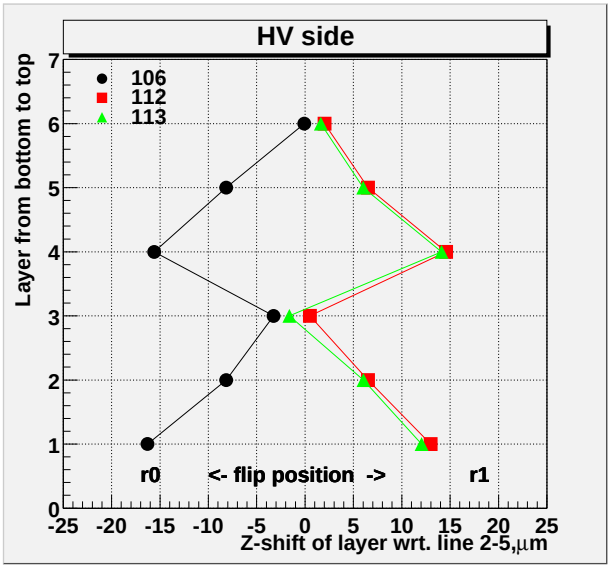

Figure 16: Shift of layers wrt. line across 2 layers wires, HV side

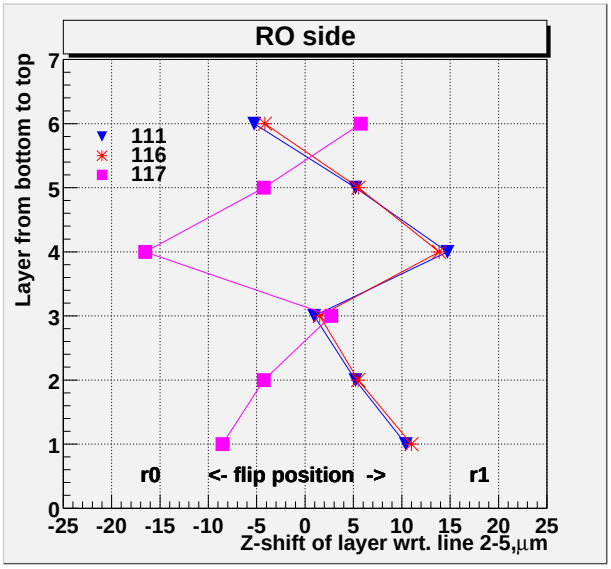

Figure 17: Shift of layers wrt. line across 2 layers wires, RO side

Table 10: Pitch for MLs

Scan	106	112	113	111	116	117
ML1 Z-pitch-30mm, μm	35.1	35.7	35.7	36.9	36.8	36.5
ML2 Z-pitch-30mm,μm	34.9	34.6	34.6	36.0	35.9	36.1
Diff. 1-2 μm	0.2	1.1	1.1	0.9	0.9	0.4

13 Z-pitches

13.1 Transverse bending influence

Transverse bending leads to compression of top multi-layer and expansion of bottom one. Difference of lengths (ML1-ML2) is equal to $Y_{ML} \cdot 4 \cdot S/W$, where Y_{ML}=252mm - ML separation, S-transverse sag of the chamber, W=1500mm - width of the chamber. For average sag=23.4μm we have lengths difference 30 μm or pitch difference 0.64 μm. Summary of grid-fit results for Z-pitch is shown in Table.10 Average difference of the z-pitch between top and bottom multi-layers is $0.77 \pm 0.34(RMS)$ μm which in good agreement with prediction from the transverse bending. Let us to remind about influence of temperature 0.7 μm/C^o for Z-pitch. It Table 1 ML1 and ML2 correspongs X-tomo scans, these are not the physical layers. Fig.18 shows dependence of the Z-pitch versus scan number for 6 layers.

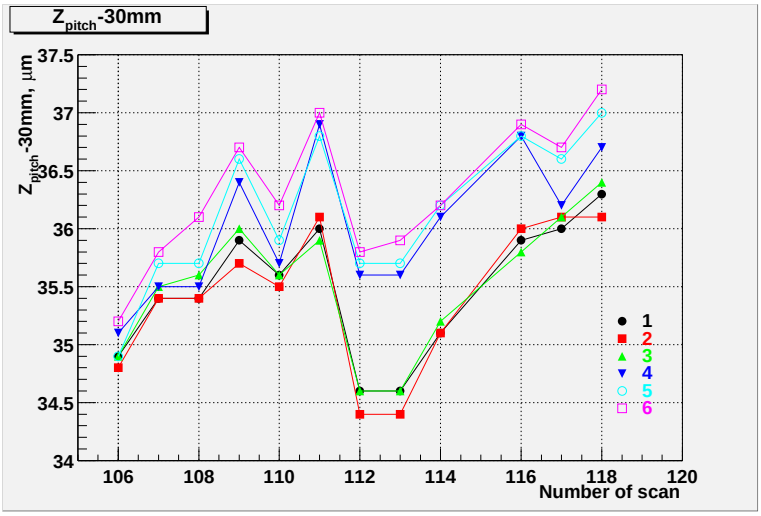

Figure 18: Z-pitch vs. scan for 6-layers

There is strange fact: for flip positions r0,r2 the Z-pitch difference between top and bottom ML is less as compare to flip r1 (see fig.18 and table 10). Such difference can not be explained by transverse sag variation.

We can suppose change of temperature difference between ML at flipping of the chamber.

For estimation of z-pitch from grid-fit results we used average for top and bottom multi-layers.

For HV side we have full agreement: nominal, design and measured X-tomo z-pitch(-30mm) 35 $\pm 0.1\mu$m.

For RO of the chamber X-tomo results shows significant difference of measured Z-pitch from designed value. As it was recognised such difference was caused by wrong alignment of the side comb. Due to significant stair length (60mm along X) small angle error leads to significant change of average Z-pitch due to accumulation of errors at the stair boundaries. This was already seen in fig.6 for Z-distributions. After assembling of the chamber the combs were re-measured. For average Z-pitch of RO side we have:

- average of the 10th grid-fit for scans 111,116,117 gives 36.30$\pm$0.15 μm;
- from layer fit with step-function we have z-pitch within a step 34.6$\pm$0.15 μm plus accumulated shift at boundaries of the stairs gives 50μm/48 as result efficient pitch is 35.6$\pm$0.2μm;
- re-measurement brings efficient pitch 35.75$\pm$0.5μm.

14 Relative angles of multi-layers

For scan 106 grid fit gives 23 μradian angle between layers at HV side. The values is explained by our fall during the chamber lifting, which lead to "kink" of distance between multi-layers at the longest chamber side of last stair (see fig.13). Simple linear fit gives us 25 μrad angle.

For another scans near the ends of the chamber we have the angles less than 12 μradian, which ought be explained by presence of bad wires. It can be analysed with using DB of wire tension, but we did not perform it.

15 Comparison of X-tomo and our data

Comparison of the producers chamber parameters with X-tomo measurements is given in table 11. In the lowest 8 rows errors of measured results are not indicated, typically they are within 1-2.5 μm.

There is a "black" sport - multi-layer shift. Due to contribution of longitudinal bending into Z-shift of layers we have not simple explanation of results. Conservative estimation - ML shift at RO about 10μm. The value which extracted from X-tomo data contents at least 3 contributions: 1) contribution due to longitudinal bending, contribution due to shift of Z-shift of origin (start position) of the layer and contribution due to relative difference of z-pitch for layers. At flipping of the chamber two last contributions changes places and the 1st one change sign. Picture becomes very complicated and has not unique interpretation.

16 Discussion and conclusions

EOL3 M0 was successfully measured at X-ray tomography.

From analysis of the chamber results we can conclude that X-tomo resolution of wire in the chamber is 2.2 μm for top and 4.2 μm for bottom multi-layers. There is systematic errors ± 2.5 μm, as we think, caused by variation of temperature.

It was recognised that at analysis of X-tomo measurements data for a long trapezoidal end cap chamber follow aspects must be taken into account (in brackets- numerical values for EOL3 M0):

- Wire grid in YZ-plane looks like stair-case parallelogram due to wire sag difference (62μ from the 1st stair to last);
- "Saw"-like shape which Y-coordinates of wires follow due to the longitudinal chamber bending and presence of "free" unsupported ends of tube (50 μm height of tooth);

Table 11: Comparison of the chamber parameters

Parameter name	Design	Meas. (producer)	Meas.(X-tomo)	Diff.(P-X-tomo)
HV $Z_{pitch} - 30mm, \mu$m	35	35±0.5	35±0.1	0
RO $Z_{pitch} - 30mm, \mu$m	35	35.8±0.5(*)	36.3±0.15	-0.5
HV ML separation-199.96mm,μm	0	0^{+10}_{-20}	-4±2.5	4.0
RO ML separation-199.96mm,μm	0	0^{+10}_{-20}	0.±1.0	0.0
HV Z-shift of MLs,μm	0	-10	0(?)	-10
RO Z-shift of MLs,μm	0	-10	10(?)	-20
HV middle layer Z-shift+15mm,μm	17.5	16	14	2
RO middle layer Z-shift+15mm,μm	17.5	22	24	-2
HV dY layer (1-3)-52mm,μm	22	23.5	18	5.5
RO dY layer (1-3)-52mm,μm	22	21.5	19	2.5
HV dY layer (1-2)-26mm,μm	12	10	6	4
HV dY layer (2-3)-26mm,μm	12	13.5	11.5	2.5
RO dY layer (1-2)-26mm,μm	12	10.5	11.5	-1
RO dY layer (2-3)-26mm,μm	12	13	15	-2

*-measured after finishing of the chamber.
Errors in last 8 rows are ±2 μm
? This is "black" sport.

- Longitudinal bending leads to about 1.5 mrad inclination side tubes together with flexo of spacer; due to 14^o trapezoidal side it gives contribution into z-shift of layers(±16 μm difference between the 1st and the 3d layers);
- There is transverse bending of the chamber (23 μm sag);
- Due to the transverse sag Z-pitch of top ML top is shorter as compare to one of the bottom ML (difference is 0.77±0.34μm).

Despite of such difficulties we could evaluate from X-tomo results the most of all interesting for production site parameters, which are in good agreement with the site measurements (see Table 9). Only question still conserved at interpretation of ML Z-shift within of 10-20μm.

There is one significant fall of the chamber producers–difference of Z-pitch at RO side. It was recognised after the chamber assembling. Re-measurements of the combs gave Z-pitch of RO side more close to X-tomo results, but still there is -0.5μm difference. It means about 20μm difference of whole side width.

All others parameters measured by X-tomo and producers are in agreement within of several μm.

Comparison of different separations between layers (see tables 7,8) provides RMS in range 8.7-16.4μm (extremal cases). It proves that RMS of single wire position within a tube is below 10 μm.

17 Some lessons of the chamber shipment

The chamber was transported from Protvino to CERN by car in wooden box, horizontally, on 8 cm foam plate. Trace of the car is not known but duration of its trip was about 2 weeks.

There are not broken wires.

Three screws(M6) from 4 connecting stretching rods with cross-plates were **unscrewed** during transportation. Several tubes were slightly damaged by the rods.

More then 10 closing caps were also **unscrewed**, there were not O-rings under these caps.

Black sports raised at the tube surface in place of contact with polyethylene film covered the chamber. It was supposed that the spots are caused electrostatics.

After all of these, several problems are seen:

- Integrity of gas-distribution system during transportation. Will it gas tight?
- Careful design and testing of all screws, used on the chamber. Fixation of RASNIK elements by epoxy.
- Safety of hedgehogs and electronics, if they will be installed on the chamber?
- Electrostatic protection, especially RO-electronics.

18 Acknowledgements

We wish to thank X-tomo group at CERN for fast taking of the chamber from box, installation of the chamber at the tomograph, fast providing of results.

19 References

1. A.Borisov et al, Precision aspects of EOL3 M0. At URL:
   http://atlas.web.cern.ch/
   Atlas/project/MDT/www/mirrorprotvino/publication/draft.html
2. http://x.home.cern.ch/x/xtomo/www/Results/Protvino_2001_01/
3. J.Berbiers et al, Calibration of the X-ray Tomography, ATLAS Internal Note, ATL-COM-MUON-2001-004.
4. A.Borisov et al, Wire tension measurements of tubes EOL3 M0. At URL:
   http://atlas.web.cern.ch/
   Atlas/project/MDT/www/mirrorprotvino/publication/draft.html

20 Appendix

Below are copies of grid-fit results for more significant runs taken from X-tomo web-page[2].

Parameters and standard deviations of grid fit shifts
Scan EOL_2001_01_p1_r0_106. EOL. Protvino. January 2001.

Number of wires:	*nominal: 48 × 6 = 288*
	measured: 286 (99.3%)

Fit number	**Estimated parameters (Z_0, Y_0 and $Angle_0$ not shown)**							**Bad wires out of 3 st. dev.**	**Z St. dev., μm**	**Y St. dev., μm**	**St. dev., μm**
	dZ, μm	**dY, mm**	**dAngle, μrad**	**$Pitch_Z$ - 30 mm, in μm**		**$Pitch_{Theta}$ - 30 mm, in μm ($Pitch_Y$, in mm)**					
				ML_1	**ML_2**	**ML_1**	**ML_2**				
	Nominal Values										
	-0.0	*199.960*	*-0.0*	*35.0*		*35.0 (26.011)*					
1	*Nominal values*							-	14.7	19.3	**17.1**
2								0	14.7	19.3	17.1
3	-	199.961	-	35.0		34.1 (26.010)		-	14.8	19.3	17.2
4	-	199.961	-	35.0		34.1 (26.010)		0	14.8	19.3	17.2
5	-23.1	199.960	23.0	35.0				-	9.0	18.4	14.5
6	-23.1	199.960	23.0	35.0				0	9.0	18.4	14.5
7	-23.1	199.961	23.0	35.0		34.1 (26.010)		-	9.0	18.4	14.5
8	-23.1	199.961	23.0	35.0		34.1 (26.010)		0	9.0	18.4	14.5
9	-23.1	199.961	23.0	35.1	34.9	37.3 (26.013)	30.9 (26.008)	-	9.0	18.3	14.4
10	-23.1	199.961	23.0	35.1	34.9	37.3 (26.013)	30.9 (26.008)	0	9.0	18.3	14.4

Yuri Sedykh

Parameters and standard deviations of grid fit shifts with wire sag corrections
Scan EOL_2001_01_p1_r0_106. EOL. Protvino. January 2001.

Number of wires:	*nominal: 48 × 6 = 288*
	measured: 286 (99.3%)

Fit number	**Estimated parameters (Z_0, Y_0 and $Angle_0$ not shown)**							**Bad wires out of 3 st. dev.**	**Z St. dev., µm**	**Y St. dev., µm**	**St. dev., µm**
	dZ, µm	**dY, mm**	**dAngle, µrad**	**$Pitch_Z$ - 30 mm, in µm**		**$Pitch_{Theta}$ - 30 mm, in µm ($Pitch_Y$, in mm)**					
				ML_1	**ML_2**	**ML_1**	**ML_2**				
	Nominal Values										
	-0.0	*199.960*	*-0.0*	*35.0*		*35.0 (26.011)*					
1	*Nominal values*							-	10.8	13.2	**12.1**
2								0	10.8	13.2	12.1
3	-	199.961	-	35.0		33.9 (26.010)		-	10.8	13.2	12.1
4	-	199.961	-	35.0		33.9 (26.010)		0	10.8	13.2	12.3
5	-13.1	199.960	23.1	35.0				-	9.6	12.3	11.0
6	-13.1	199.960	23.1	35.0				0	9.6	12.3	11.0
7	-13.1	199.962	23.1	35.0		33.9 (26.010)		-	9.6	12.3	11.0
8	-13.1	199.962	23.1	35.0		33.9 (26.010)		0	9.6	12.3	11.0
9	-13.2	199.962	23.1	35.1	34.9	36.9 (26.013)	30.9 (26.008)	-	9.6	12.1	10.9
10	-13.2	199.962	23.1	35.1	34.9	36.9 (26.013)	30.9 (26.008)	0	9.6	12.1	10.9

Parameters and standard deviations of grid fit shifts
Scan EOL_2001_01_p4_r1_111. EOL. Protvino. January 2001.

Number of wires:	*nominal: 48 × 6 = 288*
	measured: 287 (99.7%)

Fit number	Estimated parameters (Z_0, Y_0 and $Angle_0$ not shown)							Bad wires out of 3 st. dev.	Z St. dev., μm	Y St. dev., μm	St. dev., μm
	dZ, μm	dY, mm	dAngle, μrad	$Pitch_Z$ - 30 mm, in μm		$Pitch_{Theta}$ - 30 mm, in μm ($Pitch_Y$, in mm)					
				ML_1	ML_2	ML_1	ML_2				
	Nominal Values										
	-0.0	*199.960*	*-0.0*	*35.0*		*35.0 (26.011)*					
1	*Nominal values*							-	30.2	24.0	**27.3**
2								0	30.2	24.0	27.3
3	-	199.959	-	36.4		37.5 (26.013)		-	22.9	24.0	23.4
4	-	199.959	-	36.4		37.5 (26.013)		0	22.9	24.0	23.4
5	41.9	199.961	-2.3	36.4				-	12.1	23.3	18.6
6	41.9	199.961	-2.3	36.4				0	12.1	23.3	18.6
7	41.9	199.959	-2.3	36.4		37.5 (26.013)		-	12.1	23.3	18.6
8	41.9	199.959	-2.3	36.4		37.5 (26.013)		0	12.1	23.3	18.6
9	42.3	199.959	-2.3	36.9	36.0	35.3 (26.011)	39.8 (26.015)	-	10.2	23.3	18.0
10	42.3	199.959	-2.3	36.9	36.0	35.3 (26.011)	39.8 (26.015)	0	10.2	23.3	18.0

Yuri Sedykh

Parameters and standard deviations of grid fit shifts with wire sag corrections
Scan EOL_2001_01_p4_r1_111. EOL. Protvino. January 2001.

Number of wires:	*nominal: 48 × 6 = 288*
	measured: 287 (99.7%)

Fit number	**Estimated parameters (Z_0, Y_0 and $Angle_0$ not shown)**							**Bad wires out of 3 st. dev.**	**Z St. dev., µm**	**Y St. dev., µm**	**St. dev., µm**
	dZ, µm	**dY, mm**	**dAngle, µrad**	**$Pitch_Z$ - 30 mm, in µm**		**$Pitch_{Theta}$ - 30 mm, in µm ($Pitch_Y$, in mm)**					
				ML_1	**ML_2**	**ML_1**	**ML_2**				
	Nominal Values										
	-0.0	*199.960*	*-0.0*	*35.0*		*35.0 (26.011)*					
1	*Nominal values*							-	26.6	14.8	**21.6**
2								1	26.4	14.7	21.4
3	-	199.959	-	36.4		37.6 (26.013)		-	17.8	14.6	16.3
4	-	199.959	-	36.4		37.6 (26.013)		0	17.8	14.6	16.3
5	28.0	199.961	-2.6	36.4				-	12.4	14.2	13.3
6	28.0	199.961	-2.6	36.4				0	12.4	14.2	13.3
7	28.0	199.959	-2.7	36.4		37.6 (26.013)		-	12.4	14.2	13.3
8	28.0	199.959	-2.7	36.4		37.6 (26.013)		0	12.4	14.2	13.3
9	28.3	199.959	-2.6	36.9	36.0	35.4 (26.012)	39.8 (26.015)	-	10.6	14.1	12.5
10	28.3	199.959	-2.6	36.9	36.0	35.4 (26.012)	39.8 (26.015)	0	10.6	14.1	12.5

Parameters and standard deviations of grid fit shifts with wire sag corrections
Scan EOL_2001_01_p1_r1_112. EOL. Protvino. January 2001.

Number of wires:	*nominal: 48 × 6 = 288*
	measured: 286 (99.3%)

Fit number	**Estimated parameters (Z_0, Y_0 and $Angle_0$ not shown)**							**Bad wires out of 3 st. dev.**	**Z St. dev., µm**	**Y St. dev., µm**	**St. dev., µm**
	dZ, µm	**dY, mm**	**dAngle, µrad**	**$Pitch_Z$ - 30 mm, in µm**		**$Pitch_{Theta}$ - 30 mm, in µm ($Pitch_Y$, in mm)**					
				ML_1	**ML_2**	**ML_1**	**ML_2**				
	Nominal Values										
	-0.0	*199.960*	*-0.0*	*35.0*		*35.0 (26.011)*					
1	*Nominal values*							-	14.4	17.1	**15.8**
2								0	14.4	17.1	15.8
3	-	199.954	-	35.1		31.6 (26.008)		-	14.3	15.8	15.1
4	-	199.954	-	35.1		31.6 (26.008)		0	14.3	15.8	15.1
5	-11.0	199.948	-8.6	35.1				-	13.3	15.8	14.6
6	-11.0	199.948	-8.6	35.1				0	13.3	15.8	14.6
7	-11.1	199.954	-8.6	35.1		31.6 (26.008)		-	13.3	15.6	14.5
8	-11.1	199.954	-8.6	35.1		31.6 (26.008)		0	13.3	15.6	14.5
9	-10.9	199.954	-8.5	35.7	34.6	30.1 (26.007)	33.1 (26.009)	-	10.5	15.6	13.3
10	-10.9	199.954	-8.5	35.7	34.6	30.1 (26.007)	33.1 (26.009)	0	10.5	15.6	13.3

Parameters and standard deviations of grid fit shifts with wire sag corrections
Scan EOL_2001_01_p1_r1_113. EOL. Protvino. January 2001.

Number of wires:	*nominal: 48 × 6 = 288*
	measured: 285 (99.0%)

Fit number	**Estimated parameters (Z_0, Y_0 and $Angle_0$ not shown)**							**Bad wires out of 3 st. dev.**	**Z St. dev., µm**	**Y St. dev., µm**	**St. dev., µm**
	dZ, µm	**dY, mm**	**dAngle, µrad**	**$Pitch_Z$ - 30 mm, in µm**		**$Pitch_{Theta}$ - 30 mm, in µm ($Pitch_Y$, in mm)**					
				ML_1	**ML_2**	**ML_1**	**ML_2**				
	Nominal Values										
	-0.0	*199.960*	*-0.0*	*35.0*		*35.0 (26.011)*					
1	*Nominal values*							-	14.2	17.0	**15.7**
2								0	14.2	17.0	15.7
3	-	199.952	-	35.1		32.3 (26.009)		-	14.1	15.7	14.9
4	-	199.952	-	35.1		32.3 (26.009)		0	14.1	15.7	14.9
5	-9.1	199.947	-8.2	35.1				-	13.3	15.7	14.6
6	-9.1	199.947	-8.2	35.1				0	13.3	15.7	14.6
7	-9.1	199.952	-8.4	35.1		32.2 (26.009)		-	13.4	15.5	14.5
8	-9.1	199.952	-8.4	35.1		32.2 (26.009)		0	13.4	15.5	14.5
9	-8.8	199.952	-8.3	35.7	34.6	30.8 (26.007)	33.7 (26.010)	-	10.6	15.5	13.3
10	-8.8	199.952	-8.3	35.7	34.6	30.8 (26.007)	33.7 (26.010)	0	10.6	15.5	13.3

Parameters and standard deviations of grid fit shifts with wire sag corrections
Scan EOL_2001_01_p4_r1_116. EOL. Protvino. January 2001.

Number of wires:	*nominal: 48 × 6 = 288*
	measured: 282 (97.9%)

Fit number	**Estimated parameters (Z_0, Y_0 and $Angle_0$ not shown)**							**Bad wires out of 3 st. dev.**	**Z St. dev., µm**	**Y St. dev., µm**	**St. dev., µm**
	dZ, µm	**dY, mm**	**dAngle, µrad**	**$Pitch_Z$ - 30 mm, in µm**		**$Pitch_{Theta}$ - 30 mm, in µm ($Pitch_Y$, in mm)**					
				ML_1	**ML_2**	**ML_1**	**ML_2**				
	Nominal Values										
	-0.0	*199.960*	*-0.0*	*35.0*		*35.0 (26.011)*					
1	*Nominal values*							-	24.9	14.2	**20.3**
2								2	24.5	14.2	20.0
3	-	199.960	-	36.3		37.7 (26.013)		-	17.3	14.0	15.7
4	-	199.960	-	36.3		37.7 (26.013)		0	17.3	14.0	15.7
5	25.9	199.962	-1.4	36.3				-	12.6	13.6	13.1
6	25.9	199.962	-1.4	36.3				0	12.6	13.6	13.1
7	25.9	199.960	-1.5	36.3		37.7 (26.013)		-	12.6	13.6	13.1
8	25.9	199.960	-1.5	36.3		37.7 (26.013)		0	12.6	13.6	13.1
9	26.0	199.960	-1.4	36.8	35.9	35.2 (26.011)	40.1 (26.016)	-	10.7	13.5	12.2
10	26.0	199.960	-1.4	36.8	35.9	35.2 (26.011)	40.1 (26.016)	0	10.7	13.5	12.2

Parameters and standard deviations of grid fit shifts with wire sag corrections
Scan EOL_2001_01_p4_r2_117. EOL. Protvino. January 2001.

Number of wires:	*nominal: 48 × 6 = 288*
	measured: 286 (99.3%)

Fit number	**Estimated parameters (Z_0, Y_0 and $Angle_0$ not shown)**							**Bad wires out of 3 st. dev.**	**Z St. dev., µm**	**Y St. dev., µm**	**St. dev., µm**
	dZ, µm	**dY, mm**	**dAngle, µrad**	**$Pitch_Z$ - 30 mm, in µm**		**$Pitch_{Theta}$ - 30 mm, in µm ($Pitch_Y$, in mm)**					
				ML_1	**ML_2**	**ML_1**	**ML_2**				
	Nominal Values										
	-0.0	*199.960*	*-0.0*	*35.0*		*35.0 (26.011)*					
1	*Nominal values*							-	23.6	15.8	**20.1**
2								3	22.8	15.7	19.6
3	-	199.962	-	36.3		38.9 (26.014)		-	15.6	14.9	15.3
4	-	199.962	-	36.3		38.9 (26.014)		0	15.6	14.9	15.3
5	15.4	199.967	11.9	36.3				-	13.7	14.5	14.1
6	15.4	199.967	11.9	36.3				0	13.7	14.5	14.1
7	15.4	199.962	11.9	36.3		38.9 (26.015)		-	13.7	14.4	14.1
8	15.4	199.962	11.9	36.3		38.9 (26.015)		0	13.7	14.4	14.1
9	15.4	199.962	11.9	36.5	36.1	42.5 (26.018)	35.2 (26.011)	-	13.4	14.2	13.8
10	15.4	199.962	11.9	36.5	36.1	42.5 (26.018)	35.2 (26.011)	0	13.4	14.2	13.8